Available online at www.sciencedirect.com
ScienceDirect
Journal of Solid State Chemistry 180 (2007) 695–701
JOURNAL OF SOLID STATE CHEMISTRY
www.elsevier.com/locate/jssc

Hydrophilic and hydrophobic nano-sized Mn_3O_4 particles

Pierre Gibot*, Lydia Laffont

Laboratoire de Réactivité et Chimie des Solides CNRS UMR 6007, Université de Picardie Jules Verne, 33 rue Saint Leu, Amiens, F-80039, France

Received 28 August 2006; received in revised form 7 November 2006; accepted 19 November 2006
Available online 22 November 2006

Abstract

Mn_3O_4 Hausmanite nanoparticles were prepared in aqueous solution by using metallic salt and hydrazine as precursor and reducing agent, respectively. The crystallite sizes ranged from 10 to 20 nm and the particle diameter distribution was very narrow and estimated between 20 and 30 nm. Influence of some parameters such as temperature, time of reaction, surfactant nature was studied for a synthesis in an aqueous medium. The as-made manganese oxides particles could be dispersed in an organic solvent containing stabilizing agents, according to perform the synthesis in an H_2O/*n*-hexan two-phase medium. These nanoparticles were characterized by X-ray diffraction, infrared spectroscopy, scanning and transmission electron microscopies and nitrogen absorption measurements.

Keywords: Mn_3O_4; Nanoparticles; Hydrophilic; Hydrophobic

1. Introduction

Manganese oxide (Mn_3O_4, trimanganese tetroxide, Hausmannite) is currently used in many industrial application domains as catalysis, magnetism, electrochemistry or air decontamination. For example, Mn_3O_4 is a common catalyst for the oxidation of methane and carbon monoxide [1], the selective reduction of nitrobenzene [2], the decomposition of nitrogen oxides [3–5] and the oxydehydrogenation of alcohols [6]. In magnetic applications, Mn_3O_4 enables to produce soft magnetic materials such as manganese zinc ferrite which is used for magnetic cores in transformers for power supplies [7]. Trimanganese tetroxide is also used in electrochemistry as a precursor in the synthesis of Li–Mn–O electrode materials for rechargeable lithium batteries [8–12]. Finally, in air-purification applications, Hausmannite powder is able to combust organic compounds in the 100–500 °C temperature range [13,14].

In order to offer better performances due to its size and/or its morphology toward these applications, Mn_3O_4 is prepared following various methods: (i) calcination of manganese oxides (MnO_2, Mn_2O_3, etc.), oxyhydroxide (γ-MnOOH), carbonate ($MnCO_3$) and nitrate ($Mn(NO_3)_2$) at high temperature (1000 °C) [15–17], (ii) solvothermal treatment of manganite (MnOOH) [18–23] (iii) sol–gel process with a post-treatment at higher temperature [24,25], (iv) precipitation coupled with oxidation of manganese hydroxide ($Mn(OH)_2$) [26] (v) electrospinning technique [27,28] and (vi) gas condensation [29]. More recently, other Mn_3O_4 synthetic process are investigated: (vii) chemical bath deposition to prepare thin films [30] (viii) gamma-ray irradiation of manganese sulfate ($MnSO_4 \cdot H_2O$) [31] and finally (ix) precipitation method from manganese nitrate ($Mn(NO_3)_2$) at moderate temperature [32].

In this paper, a novel synthesis of nano-sized Mn_3O_4 particles at room temperature in aqueous and organic reactional medium is reported. Very stable nanomaterials dispersions were obtained in some cases due to the addition of stabilizing agents. The as-made material presents a high degree of crystallinity, a monocrystalline character and a very narrow grain size distribution as demonstrated by X-ray diffraction (XRD), scanning electron microscopy (SEM) and high-resolution transmission microscopy (HRTEM) characterizations.

2. Experimental section

The synthesis was performed under atmospheric conditions with commercially available reagents without further

*Corresponding author. Fax: +33 3 2282 7590.
E-mail address: Pierre.gibot@u-picardie.fr (P. Gibot).

0022-4596/$ - see front matter © 2006 Elsevier Inc. All rights reserved.
doi:10.1016/j.jssc.2006.11.024

purification. Absolute ethanol, *n*-hexan (98.5%), potassium permanganate $KMnO_4$ (99 + %), monohydrate hydrazine $N_2H_4 \cdot H_2O$ (98%), cetyltetramethylammonium bromide (CTAB) and stabilizing reagents such as oleylamine (OE-70%) were purchased from Aldrich Chemical Co. Surfactant reagent like sodium dodecylsulfate (SDS) was obtained from Acros Organics.

2.1. Synthesis of hydrophilic Mn_3O_4 nanoparticles

$KMnO_4$ (4×10^{-4} mol) were dissolved into 20 ml of distilled water. For systems containing surfactants, 4×10^{-4} mol of SDS or CTAB were added once to aqueous metallic solution and the mixtures were homogenized during a few minutes under slowly stirring (in order to avoid foam formation). Then, 20 ml of an aqueous solution of monohydrate hydrazine (4×10^{-3} mol) was injected rapidly to the salt/surfactant solution (pH = 9,H_2SO_4 1 M) under vigorous magnetic stirring. The colour of the solution immediately turned from dark purple to black/brown then to orange/brown. The system was kept at room temperature or heated at 70 °C from fifteen minutes to 1 h and cooled down to room temperature by removing the heat source. An orange/brown material was precipitated and separated via centrifugation. The solid was washed twice with distilled water then once with ethanol and dried at 50 °C overnight.

2.2. Synthesis of hydrophobic Mn_3O_4 nanoparticles

The synthesis was performed in an H_2O/*n*-hexan two-phase medium. The surfactant in aqueous solution was sodium dodecylsulfate. Thirty milliliter of organic phase as *n*-hexan containing 1 vol% of stabilizing agent, i.e. oleylamine was added to the aqueous mixture before heating. At the end of the reaction, an orange coloured organic phase was obtained. The colourless aqueous phase was discarded. The orange/brown solid was washed, centrifugated and dried before characterizations.

2.3. Nanoparticles characterization

X-ray powder diffraction patterns of the Mn_3O_4 nanoparticles were collected on a Philips PW 1830 diffractometer with a Cu $K\alpha$ radiation ($\lambda = 1.54056$ Å), operating at 40 kV and 30 mA. Crystallographic data (lattice parameters, space groups) have been determined by using WinPLOTR software.

Infrared spectra of studied samples were obtained using a Nicolet 510 FTIR spectrometer equipped with a KBr beam splitter and a DTGS detector. Spectra were recorded in the wavenumber range 4000–400 cm^{-1} by addition of 100 scans and with a resolution of 4 cm^{-1}. The spectra were recorded in the transmission mode.

The morphology of the transition metal oxides nanoparticles was investigated by SEM (Philips FEG XL-30). A metalsprayer equipment (30 mA—90 s) was used to coat a thick gold layer on samples.

Nitrogen adsorption/desorption measurements were performed on a Micromeritics ASAP 2010 at 77 K. Prior to the measurements, the samples have been outgassed at 393 K for 12 h. The specific surface area (S_{BET}) was determined according to the Brunauer–Emmet–Teller (BET) method in the relative pressure 0.02–0.25.

TEM and HRTEM imaging were performed using a FEI Tecnai F20 S-Twin electron microscope operating at 200 kV. Samples for electron microscopy analysis were prepared by depositing at room temperature a dispersion of nanoparticles on copper grids coated with lacey-carbon film. The diffraction patterns were obtained using the selected area electron diffraction (SAED) mode or by Fourier transform of the HRTEM image.

3. Results and discussion

3.1. Hydrophilic Mn_3O_4 nanoparticles characterization

The name and experimental conditions of each sample are reported in detail in Table 1.

For all experiments, a floculation appeared very rapidly just at the end of stirring except for the SDS-based preparation where a very stable orange sol was obtained. Stability of this preparation has been controled after several days. This suggests that SDS surfactant was capped around the particles and enables their good dispersibility.

The XRD patterns of the as-prepared products are presented in Fig. 1. It is difficult to distinguish between Mn_3O_4 Hausmannite (JCPDS card no 24-0734) and γ-Mn_2O_3 (JCPDS card no 18-0803) because the XRD patterns are very similar. Therefore, the intensity of some diffraction peaks (2θ# 28.9°; 36° and 44.4°) can enable the distinction. The crystalline phase of all the samples studied is preferentially indexed according to centered tetragonal structure with $I4_1/amd$ space group as for Mn_3O_4. No other phases are detected.

Fig. 2 shows a full pattern matching refinement results of XRD data of one of as-prepared Mn_3O_4; in particular Mn_3O_4-2. The fitting is in good agreement with the experimental XRD pattern and the lattice parameters have been determined: $a = 5.7669(4)$ Å, $c = 9.4506(4)$ Å and

Table 1
Name and experimental conditions of each prepared samples (RT = room temperature)

Name	T (°C)	Time (min)	Surfactant
Mn_3O_4-1	70	15	—
Mn_3O_4-2	70	60	—
Mn_3O_4-3	RT	15	—
Mn_3O_4-4	RT	60	—
Mn_3O_4-C	70	60	CTAB
Mn_3O_4-S	70	60	SDS

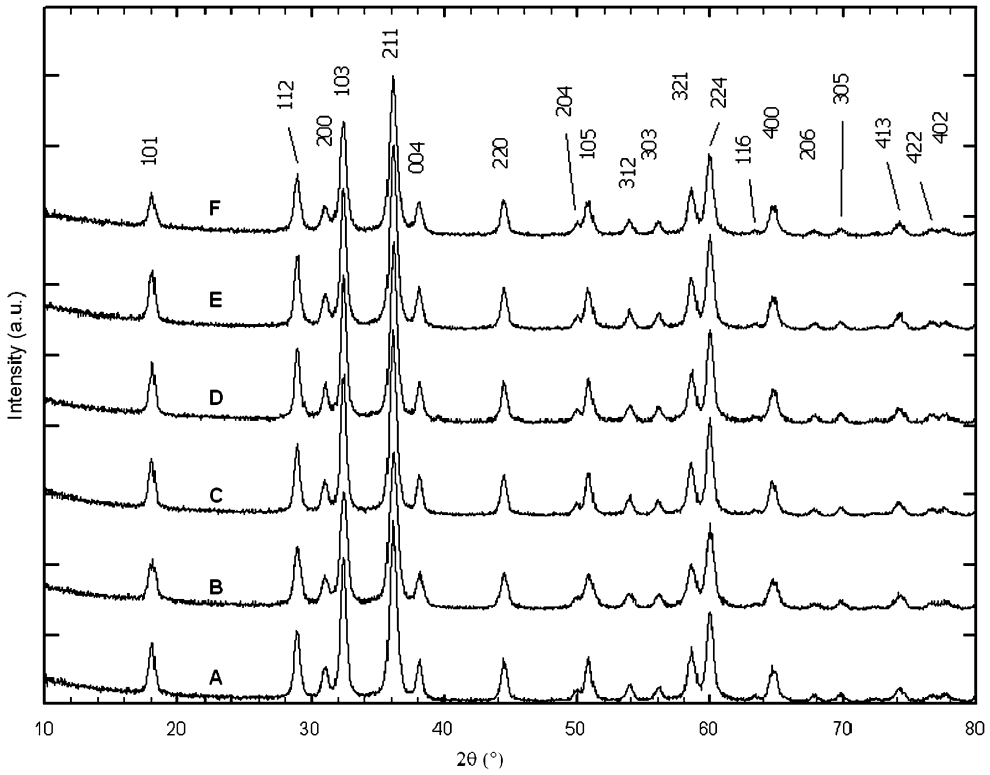

Fig. 1. X-ray diffraction patterns of (A) Mn_3O_4-1, (B) Mn_3O_4-2, (C) Mn_3O_4-3, (D) Mn_3O_4-4, (E) Mn_3O_4-C and (F) Mn_3O_4-S samples. Samples were deposited on glass substrates.

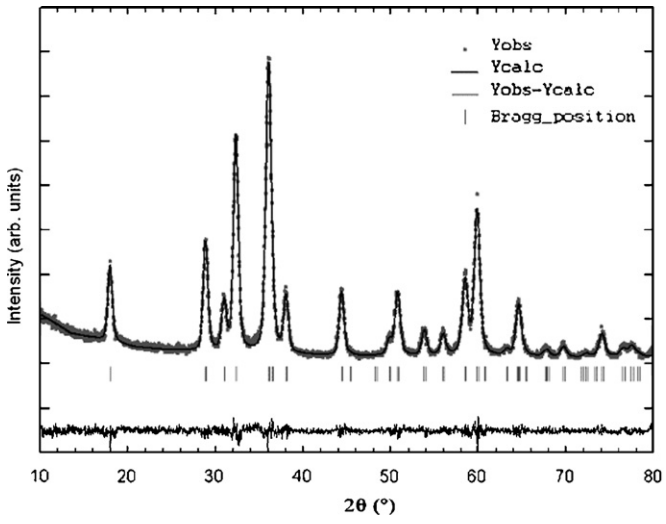

Fig. 2. Full pattern matching refinement results of Mn_3O_4-2 samples.

$V = 314.30(5)\,Å^3$ ($R_{wp} = 10.1 - R_{exp} = 8.75$). The crystallite size of Mn_3O_4-2, calculated from the refinement and a reference sample such as LaB_6 analyzed in the same experimental conditions, is 147.50 Å with a standard deviation of 16.25 Å. This weak standard deviation might suggest an isotropic crystallite such as a nano-sphere.

To confirm the chemical nature of the as-made nanomaterials, infrared spectroscopy was used. Fig. 3 shows the FTIR spectra of some as-prepared samples: Mn_3O_4-2 (A), Mn_3O_4-C (B) and Mn_3O_4-S (C) and the sodiumdodecylsulphate surfactant (D). Three absorption peaks are observed from 400 to 650 cm^{-1} for sample A, B and C; vibration frequency at 635–638 cm^{-1} is characteristic of Mn–O stretching modes in tetrahedral sites [33] whereas vibration frequency at 534–536 cm^{-1} corresponds to the distortion vibration of Mn–O in an octahedral environment [33]. The third vibration band, located at a weaker wavenumber, i.e. 417–418 cm^{-1}, can be attributed to the vibration of manganese species (Mn^{3+}) in an octahedral site [33]. This spectroscopic domain enables to eliminate the formation of γ-Mn_2O_3 due to the absence of one of its primordial vibration bands located at 670 cm^{-1} [34]. For all spectra, characteristic bands for OH bond in water, around 3400–3500 and 1633 cm^{-1}, corresponding to adsorption of water at the nanoparticle surface are detected.

FTIR spectra of Mn_3O_4-C (B), i.e. prepared from surfactant such as CTAB (Fig. 3), no vibration bands relating to the surfactant (vibration bands of $-CH_2$, $-CH_3$, $-NH_4^+$, etc) are detected; indicating that the as-prepared Mn_3O_4 surface is free of this molecule. On the contrary for Mn_3O_4 prepared from SDS surfactant (Fig. 3C), vibrations bands coming from sodiumdodecylsulphate (Fig. 3D) are clearly seen. The difference between these characteristic peaks is either the peak intensity or shift of the peak position. For example, the peaks of the SDS surfactant located at 1102–1210 and 618 cm^{-1}, corresponding to the vibration mode of SO_3^-, shift to lower wavenumbers (1025–1160 cm^{-1}) or disappear, after

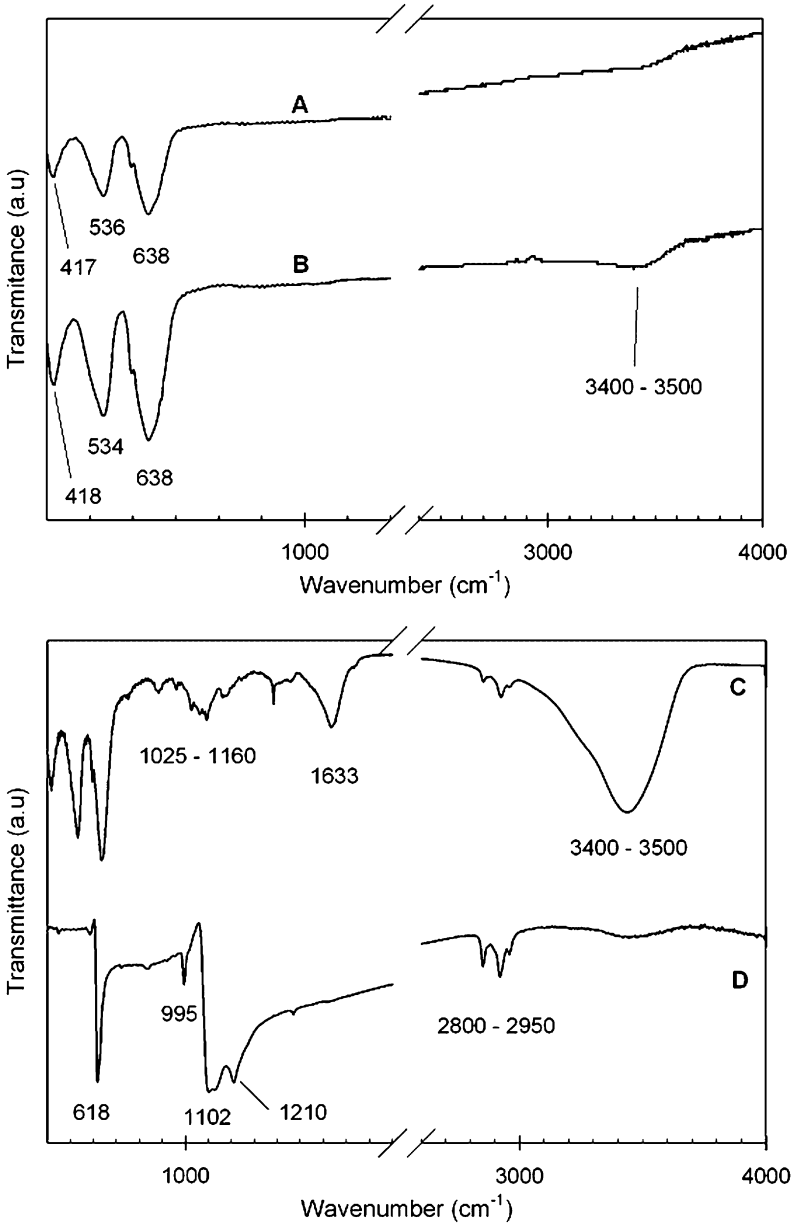

Fig. 3. FTIR spectra of hydrophilic (A) Mn_3O_4-2 , (B) Mn_3O_4-C and (C) Mn_3O_4-S nanoparticles and (D) sodiumdodecylsulfate.

its adsorbtion on the surface of the manganese oxide particles (Fig. 3C). This phenomena is probably due to a decrease in their mobility explained by the formation of a very compact surfactant layer on the nanoparticles surface [35]. Finally the vibrations bands of alkyl groups ($-CH_2-CH_2-$, $-CH_2$, $-CH_3$) at 2800–2950 cm^{-1} in the Mn_3O_4-S spectrum (Fig. 3C) confirm the capping of sodiumdodecylsulfate on the particles surface.

In order to determine the morphology of the Mn_3O_4 particles, SEM characterizations were performed. Fig. 4 displays the SEM images of Mn_3O_4-2, Mn_3O_4-C and Mn_3O_4-S samples. For a material without surfactant (Mn_3O_4-2) (Fig. 4A) or with surfactant such as CTAB (Mn_3O_4-C/Fig. 4B), the Hausmannite nanoparticles are almost in the spherical shape with a mean diameter close to 20–30 nm. However, with addition of SDS (Fig. 4C), Mn_3O_4-S particles have a more spherical shape and a bigger size. A mean diameter of particles of 40–50 nm is estimated relating to a slightly aggregation of crystallites. In fact, a crystallite size equal to 125.52 Å with a standard deviation of 6.42 Å was determined by a full pattern matching refinement of the XRD pattern (not shown here). To determinate more precisely the average particle size for all the prepared samples, BET surface areas measurement was performed. BET specific surface areas, with corresponding average particle size, are listed in Table 2. The average particle size was calculated with the formula:

$$\emptyset = 6/(\rho \times S), \quad (1)$$

where ρ is the theorical density of the Mn_3O_4 material (4876 kg m^{-3}) and S is the specific surface area of the studied nanomaterial. The size of nanoparticles determined

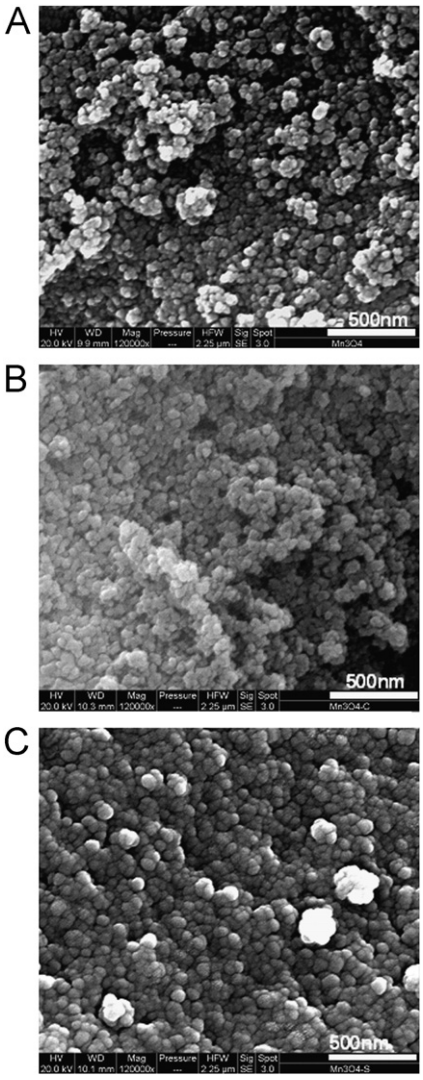

Fig. 4. SEM pictures of hydrophilic (A) Mn_3O_4-2, (B) Mn_3O_4-C and (C) Mn_3O_4-S nanoparticles.

Table 2
BET surface area and relating average particle size of Mn_3O_4 nanospheres

Name	SBET ($m^2 g^1$)	Ø (nm)
Mn_3O_4-1	72	17
Mn_3O_4-2	68	18
Mn_3O_4-3	66	19
Mn_3O_4-4	62	20
Mn_3O_4-C	68	18
Mn_3O_4-S	28	44

by the method is in good agreement with those estimated by SEM characterizations and calculated from XRD; in particular for Mn_3O_4-2 and Mn_3O_4-C. For Mn_3O_4-S an aggregation of nano-crystallites is confirmed.

TEM and HRTEM were performed on the hydrophilic Mn_3O_4 samples to determine their structure and nanostructure. Fig. 5 shows the TEM pictures of (A) Mn_3O_4-C and (B) Mn_3O_4-S combined with the diffraction patterns obtained in SAED mode. The two bright-field images show that Mn_3O_4-C and -S are composed of nanoparticles with a spherical shape (the same image is observed for Mn_3O_4-2). The associated diffraction patterns confirm that the samples are Mn_3O_4 Hausmannite (JCPDS card no 24-0734—space group $I4_1/amd$). Opposite to Mn_3O_4-2 and -C, Mn_3O_4-S (Fig. 5B) presents a layer which is surrounded by the nanoparticles. This layer, highlighted in Fig. 6 by the black arrows, is amorphous with a size of 1–2 nm. In order to characterize precisely these samples, HRTEM pictures of the nano-sized manganese oxides were realized. About Mn_3O_4-2 and Mn_3O_4-S nanoparticles, the images (Fig. 6A and B) reveal spherical particles with 10–20 and 10–30 nm size, respectively. These nanoparticles present a high crystallinity degree that emphasizes the monocrystalline characters of the studied nanomaterial. The behaviour of Mn_3O_4-C sample (prepared with CTAB-HRTEM picture not shown here) is equivalent to Mn_3O_4 prepared without surfactant; i.e. Mn_3O_4-2.

3.2. Hydrophobic Mn_3O_4 nanoparticles characterization

These nanomaterials were prepared from a two-phase medium. They are very soluble in *n*-hexan producing an orange organosol which seems to be stable for months without deposit of solid matter in the recipient. This dispersion phenomenon is similar to those of Mn_3O_4-S where sodium dodecylsulsulfate stabilizing agent is substituted for oleylamine (OE). The as-made nanomaterials are identified as Mn_3O_4 nanoparticles as reported by the XRD pattern of Fig. 7 (sample named Mn_3O_4-OE). Crystallographic data are the following : $a = 5.7679(3)$ Å, $c = 9.4324(3)$ Å and $V = 313.80(8)$ Å^3 ($R_{wp} = 9.28-$ $R_{exp} = 8.56$) with a cristallite size close to 68.75 Å and a standard deviation of 5.87 Å.

To better understand the adsorption process of the oleylamine on the surface of Mn_3O_4 nanoparticles, infrared measurements were performed on the pure oleylamine (OE) surfactant and the manganese oxide particles grafted with oleylamine; their spectra are reported in Fig. 8A and B, respectively. About Mn_3O_4 nanoparticles capped with oleylamine surfactant, i.e Mn_3O_4-OE (Fig. 8A), the vibration band characteristics of ''manganese oxide'' are located at 420, 530 and 634 cm^{-1}. The assignments of the other vibrations bands which are well established in the literature [36] are presented in Table 3. Comparing the two spectra, two new vibration bands are detected on spectrum B; at 970 and 3070 cm^{-1}. Those can be attributed to the stretching of the C–H bond adjacent to the C=C double bond and might correspond to a conversion of oleylamine in elaidic amine, i.e. from the *cis*-form to the *trans*-form, as explained by Shukla et al. [36].

TEM image of the as-prepared Mn_3O_4-OE nanoparticles (Fig. 9A) shows monodispersed and isolated particles with 5–10 nm size without specific shape. The HRTEM picture (Fig. 9B) shows the monocrystalline character of particles. The Fourier transform of one part of HRTEM confirms the particle structure (centered tetragonal Hausmannite).

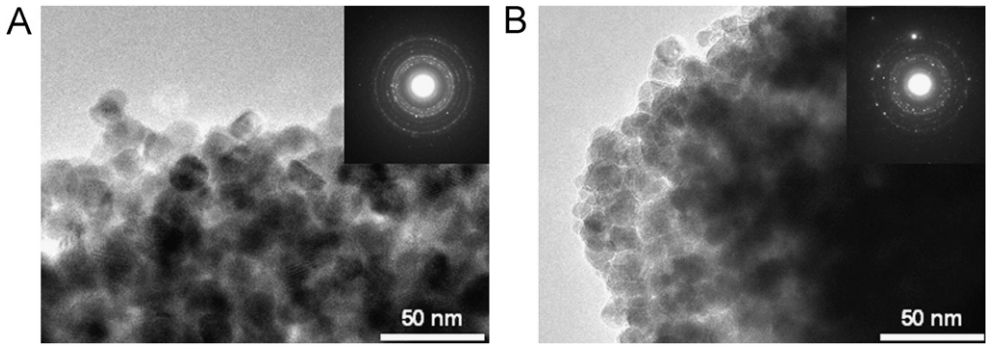

Fig. 5. TEM micrographs of hydrophilic (A) Mn_3O_4-C and (B) Mn_3O_4-S nanoparticles.

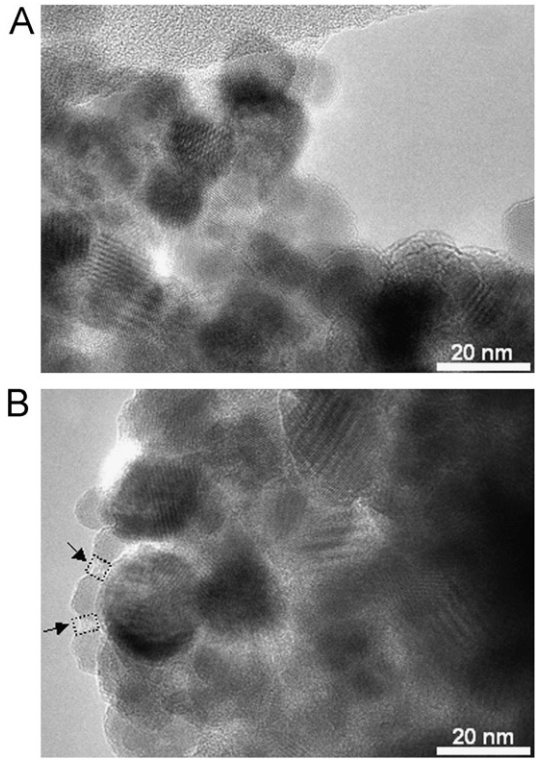

Fig. 6. HRTEM image of (A) 10–20 nm Mn_3O_4-2 nanoparticles and (B) 10–30 nm Mn_3O_4-S nanoparticles.

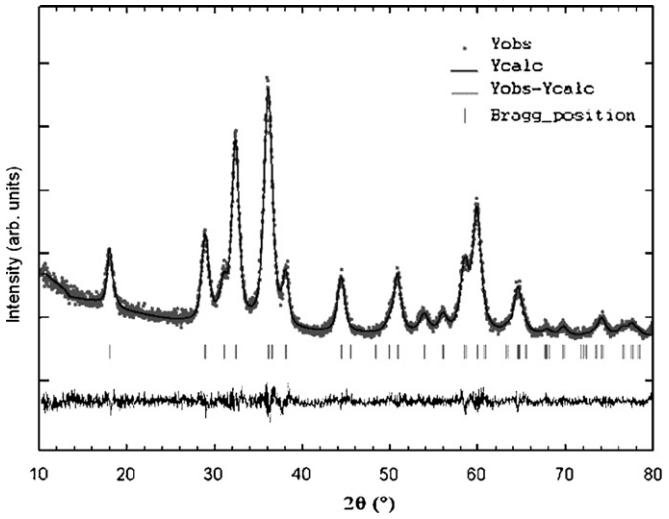

Fig. 7. Full pattern matching refinement results of Mn_3O_4-OE nanoparticles.

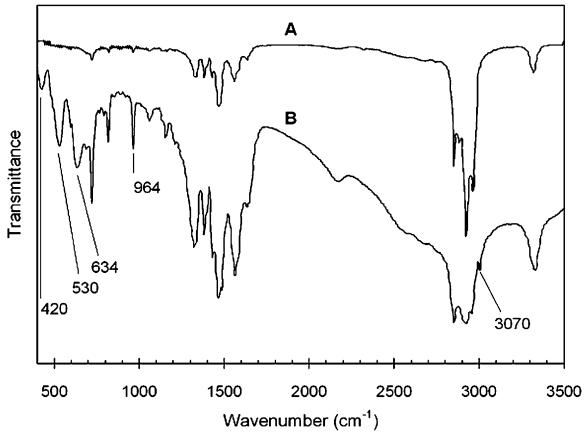

Fig. 8. FTIR spectra of (A) oleylamine surfactant (OE) and (B) hydrophobic Mn_3O_4-OE.

4. Conclusion

A novel route of synthesis of nano-sized Mn_3O_4 Hausmannite nanoparticles, at atmospheric temperature and pressure was described. This route consisted in reducing metallic salt by hydrazine in aqueous or two-phase medium; performing hydrophilic or hydrophobic nanoparticles synthesis, respectively. Based on experimental results, the particles size is ranging from 5 nm for a preparation in organic solvent to 30 nm according to a synthesis in aqueous solution with surfactants. Particles reveal a monocrystalline character and a "spherical" shape. By performing the Mn_3O_4 particles synthesis in a two-phase medium (containing a stabilizing agent) isolated and dispersed nanoparticles were obtained. Electrochemical and catalysis tests about these as-made Mn_3O_4 nanoparticles are under way in our laboratory.

Table 3
Infrared vibrational assignments

Wavenumber (cm^{-1})	Vibrational modes
721	$\delta(-CH_2-)_n$
817	γ(N–H)
1062	$\delta(-C-N)$
1151	$\gamma(-CH_2)$
1325	$\gamma(-CH_2)$
1382	$\delta_s(-CH_3)$
1440	$\delta_{as}(-CH_3)$
1466	$\delta_s(-CH_2)$
1483	$\delta_{as}(-CH_2)$
1564	δ(N–H)
1592	$\nu(NH_2)$
1640	$\nu(-C=C)$
2851	$\nu_s(-CH_2)$
2921	$\nu_{as}(-CH_2)$
2955	$\nu_{as}(-CH_3)$
3006	cis $\nu(-CH=)$
3331	ν(NH)

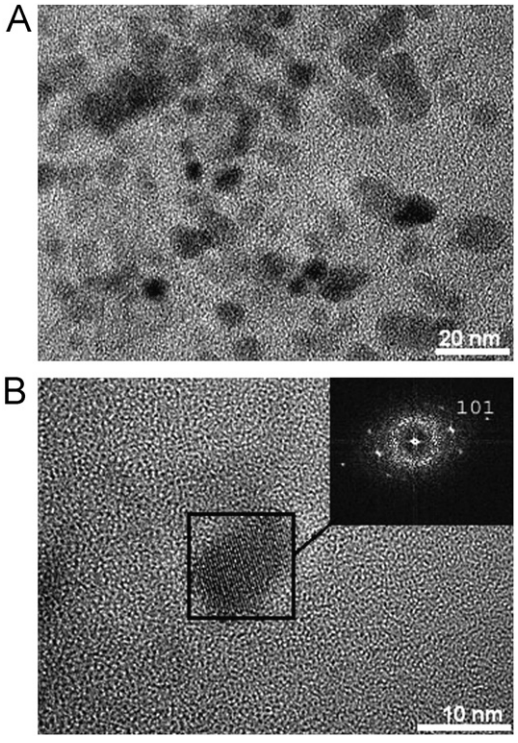

Fig. 9. (A) TEM and (B) HRTEM image of Mn_3O_4-OE nanoparticles from an *n*-hexan sols.

References

[1] E.R. Stobhe, B.A.D. Boer, J.W. Geus, Catal. Today 47 (1999) 161–167.
[2] E. Grootendorst, Y. Verbeck, V. Ponce, J. Catal. 157 (1995) 706–712.
[3] T. Yamashita, A. Vannice, J. Catal. 163 (1996) 158–168.
[4] W.M. Wang, Y.N. Yang, Z. Jiayu, Appl. Catal. A 133 (1995) 81–93.
[5] A. Maltha, H.F. Kist, B. Brunet, J. Ziolkowski, H. Onishi, Y. Iwasawa, V. Ponec, J. Catal. 149 (1995) 356–363.
[6] M. Baldi, F. Milella, G. Ramis, V. Sanchez Escribano, G. Busca, Appl. Catal. A Gen 166 (1) (1998) 75–88.
[7] V.V. Pankov, Ceram. Int. 14 (1998) 87–91.
[8] M.M. Thackeray, W.I.F. David, P.G. Bruce, Mater. Res. Bull. 18 (1983) 461–472.
[9] J.C.Z. Nardi, J. Electrochem. Soc. 132 (1985) 1787–1790.
[10] M. Wu, Q. Zhang, H. Lu, A. Chen, Solid State Ionics 169 (1–4) (2004) 47–50.
[11] V. Berbenni, A. Marini, J. Anal. Appl. Pyrol. 70 (2) (2003) 437–456.
[12] S. Komaba, S.-T. Myung, N. Kumagai, T. Kanouchi, K. Oikawa, T. Kamiyama, Solid State Ionics 152–153 (2002) 311–318.
[13] M. Baldi, E. Finocchio, F. Milella, Appl. Catal. B. Environ. 16 (1998) 43–51.
[14] M.F.M. Zwinkels, S.G. Jaras, P.G. Menon, Catal. Rev. Sci. Eng. 35 (1993) 319–324.
[15] C.H. Shomate, J. Am. Chem. Soc. 65 (1943) 786–790.
[16] J.C. Southard, G.E. Moore, J. Am. Chem. Soc. 64 (1942) 1769–1773.
[17] I. Ursu, R. Alexandrescu, I.N. Mihailescu, J. Phys. B 19 (1986) 825–829.
[18] Y.C. Zhang, T. Qiao, X.Y. Hu, J. Solid State Chem. 177 (2004) 4093–4097.
[19] G. Demazeau, J. Mater. Chem. 9 (1999) 15–18.
[20] M. Yoshimura, MRS Bull. Special Issue 25 (2000) 17–25.
[21] R.I. Walton, Chem. Soc. Rev. 31 (2002) 230–238.
[22] Y.Q. Chang, X.Y. Xu, X.H. Luo, C.P. Chen, D.P. Yu, J. Cryst. Growth 264 (1–3) (2004) 232–236.
[23] W. Zhang, Z. Yang, Y. Liu, S. Tang, X. Han, M. Chen, J. Cryst. Growth 263 (1–4) (2004) 394–399.
[24] S. Ching, J.L. Roark, N. Duan, Chem. Mater. 9 (1997) 750–754.
[25] F.A. AL Sagheer, M.A. Hasan, L. Pasupulety, J. Mater. Sci. Lett. 18 (1999) 209–211.
[26] Y.I. Jang, H. Wang, Y.M. Chiang, J. Mater. Chem. 8 (1998) 2761–2764.
[27] C. Shao, H. Guan, Y. Liu, X. Li, X. Yang, J. Solid State Chem. 177 (2004) 2628–2631.
[28] C.L. Shao, H.Y. Guan, Y.S.B. Wen, B. Chen, X.H. Yang, J. Gong, Chin. Chem. Lett. 15 (4) (2004) 471–474.
[29] L. Dimesso, L. Heider, H. Hahn, Solid State Ionics 123 (1–4) (1999) 39–46.
[30] H.Y. Xu, S.L. Xu, H. Wang, H. Yan, J. Electrochem. Soc. 152 (12) (2005) C803–C807.
[31] Y. Hu, J. Chen, X. Xue, T. Li, Mater. Lett. 60 (2006) 383–385.
[32] S. Rabiei, D.E. Miser, J.A. Lipscomb, K. Saoud, S. Gedevanishvili, F. Rasouli, J. Mater. Sci. 40 (2005) 4995–4998.
[33] M. Ishii, M. Nakahira, Solid State Commun. 11 (1972) 209–212.
[34] B. Gillot, M. El Guendouzi, M. Laarj, Mater. Chem. Phys. 70 (2001) 54–60.
[35] B.A. Korgel, S. Fullam, S. Connolly, D. Fitzmaurice, J. Phys. Chem. B 102 (1998) 8379–8388.
[36] N. Shukla, C. Liu, P.M. Jones, D. Weller, J. Magn. Magn. Mater. 266 (2003) 178–184.